Brenner–Gajdos theory is not correct for flexible polymers, it should be a reasonable approximation for small λ_H.
(49) Baumgärtner, A.; Muthukumar, M. *J. Chem. Phys.* **1987,** *87,* 3082.
(50) Kremer, K.; Binder, K. *J. Chem. Phys.* **1984,** *81,* 6381.
(51) van Brakel, J.; Heertjes, P. M. *Int. J. Heat Mass Transfer* **1974,** *17,* 1093.
(52) Pismen, L. M. *Chem. Eng. Sci.* **1974,** *29,* 1227.
(53) Katz, A. J.; Thompson, A. H. *Phys. Rev. Lett.* **1985,** *54,* 1325.
(54) Bohrer, M. P. *Ind. Eng. Chem. Fundam.* **1983,** *22,* 72.

Soluble Ethylmercapto-Substituted Polythiophenes

Jose P. Ruiz, K. Nayak, Dennis S. Marynick,* and John R. Reynolds*

Department of Chemistry, The University of Texas at Arlington, Arlington, Texas 76019.

Received May 17, 1988; Revised Manuscript Received September 9, 1988

ABSTRACT: Polymers of 3-(ethylmercapto)- and 3,4-bis(ethylmercapto)thiophenes have been synthesized and characterized. These polymers are soluble in common organic solvents such as methylene chloride, chloroform, and THF. Structural characterization using FT-IR and NMR spectroscopy show that these polymers have a well-defined β-(ethylmercapto)-substituted 2,5-(thienylene) polymeric structure. Visible–near-IR absorption spectra of electrochemically doped cast films and chemically doped solutions of the polymers show that they can be oxidized to form bipolaronic species. GPC studies show a number average molecular weight of about 2500 ($M_w/M_n \sim 5$) for both polymers. Maximum electrical conductivities of 10^{-3} Ω^{-1} cm^{-1} for the 3-(ethylmercapto)- and 10^{-7} for the 3,4-bis(ethylmercapto)-substituted polymers have been obtained in the oxidized state. Experimental results are correlated with theoretical calculations by using the PRDDO and extended Hückel methods, which demonstrate radical-cation reactivites for the thiophene monomers, along with minimum energy conformations and band structures in these substituted polymers.

Introduction

In the last decade, there has been considerable interest in the study of electronically conducting polymers. These efforts can be attributed to the large number of potential applications for such materials and scientific curiosity in the ability of organic materials to conduct charge.[1] The most promising of these materials should demonstrate good solution or melt processability, environmental stability, good mechanical properties, and controllable conductivities.

To improve the physical and electronic properties of these polymers, much work has been done in altering the synthetic conditions and molecular architecture of aromatic polyheterocycles, including polythiophenes, polypyrroles, and polyfurans.[2] It has been found that by placing β-position substituents on polythiophenes, highly conducting (ca. 10^{+1} Ω^{-1} cm^{-1}), yet soluble polymers are formed. Initially, Elsenbaumer et al.[3] reported a series of 3-alkylthiophene polymers that were soluble in common organic solvents. Their solubility increased with the size of the substituents, while having little effect on the maximum conductivity. Similar results have also been reported by Sato et al.[4] Due to their solubility in typical organic solvents, solution spectroscopic studies have been carried out by Heeger et al.[5,6] Recently, conducting polymers prepared from β-substituted thiophenes were reported by Bryce et al.[7] that not only are soluble but in some cases had elevated conductivities (ca. 10^{+3} Ω^{-1} cm^{-1}) relative to the unsubstituted parent, polythiophene. To date there have been two brief reports on the preparation of mercapto-substituted polythiophenes.[3,8] In both cases relatively low maximum conductivities, on the order of 10^{-1} Ω^{-1} cm^{-1}, were reported.

The ability to process these polymers using common solution processing techniques opens up a broad area of research in conductive polymers. Here we report on the synthesis and characterization of poly[3-(ethylmercapto)thiophene] (PEMT) and poly[3,4-bis(ethylmercapto)thiophene] (PBEMT), both of which are soluble in common organic solvents and semiconducting (up to 10^{-3} Ω^{-1} cm^{-1}) in the oxidized state. We correlate our structural and electronic results to results from theoretical calculations, demonstrating the ability of theory to assist in directing experimentation.

Experimental Section

Preparation of Monomers and Polymers. 3-(Ethylmercapto)thiophene (EMT) and 3,4-bis(ethylmercapto)thiophene (BEMT) were prepared from their corresponding bromo-substituted thiophenes according to the method of Yabukov et al.[9] Both materials were purified by fractional distillation in vacuo.

Different α-halogenation procedures were used for the monomers. EMT was brominated by using a published procedure for typical brominations.[10] Pure 2,5-dibromo-3-(ethylmercapto)thiophene was obtained after fractional distillation in vacuo. BEMT was iodinated employing the method of Barker et al.[11] to give 2,5-diiodo-3,4-bis(ethylmercapto)thiophene. Purification was carried out by reprecipitation from methylene chloride into methanol.

Solution polymerization of these 2,5-dihalogeno-substituted monomers was done via a nickel-catalyzed Grignard coupling similar to the procedures used by Kobayashi et al.[12] and Elsenbaumer et al.[3] As reported previously, 2-methyltetrahydrofuran was used as the Grignard formation solvent and nickel(II) bis(diphenylphosphino)propane dibromide [Ni(DPPP)Br_2] as the coupling catalyst. The polymerization was carried out under nitrogen at 130 °C for at least 70 h. The polymers were purified by reprecipitation into methanol from methylene chloride and dried under vacuum. Brick red and ochre colored powders were obtained for EMT and BEMT polymers, respectively.

Structural Identification of Monomers and Polymers. Infrared spectra were obtained by using a Digilab FTS-40 FT-IR spectrophotometer utilizing transmittance between NaCl plates for liquids and the diffuse reflectance technique (DRIFT) for solids. The DRIFT method was used instead of pressed KBr pellets due to the highly opaque nature of the polymer samples.

^{1}H NMR spectra were done on a Varian EM-360 spectrometer for all monomeric materials and a Nicolet 200 FT-NMR for polymers in deuteriated chloroform. ^{13}C NMR for all materials were obtained on the Nicolet 200 instrument.

Elemental analyses were done by Texas Analytical Laboratories (Tallahassee, FL).

Theoretical Calculations. Molecular orbital calculations were performed in order to assess the spin densities of the monomeric

0024-9297/89/2222-1231$01.50/0

Table I
Infrared Absorption Positions and Assignments for Monomeric and Polymeric Materials (cm^{-1})

	arom C–H		aliph C–H			ring stretch			methyl deformation	arom C–H out of plane
	α	β								
EMT	3101	3066	2974	2924	2870	1492	1446	1427	1373	1099, 852, 779
dibromo-EMT		3066	2974	2931	2916	1500	1446	1427	1373	825
PEMT	3090	3070	2974	2916	2867	1508	1481	1423	1373	825
BEMT	3101		2970	2924	2870	1473	1446	1427	1373	960, 856, 787
diiodo-BEMT			2974	2962	2920		1442	1423	1373	
PBEMT	3090		2968	2922	2865	1508	1489	1446	1373	
polythiophene[a]		3063				1491	1453	1441		788
poly(3-hexylthiophene)[b]		3055	2959	2930	2858	1512	1458	1439	1377	825

[a] Polythiophene synthesized in our laboratory via Kobayashi method. [b] From ref 5.

Table II
^1H NMR Chemical Shifts and Assignments for Monomeric and Polymeric Materials (ppm)

	aromatic			
compd	α-H	β-H	methylene	methyl
EMT	6.95 (m)	7.05 (d)	2.77 (q)	1.20 (t)
dibromo-EMT		6.83	2.80 (q)	1.23 (t)
PEMT	7.04 (w)	7.12	2.91, 2.50	1.57, 1.31
BEMT	7.07 (s) [6.99][a]		2.90 (q) [2.78][a]	1.30 (t) [1.23][a]
diido-BEMT			2.97 (q)	1.20 (t)
PBEMT	7.05 (w)		2.88	1.17

[a] Values in brackets by Yabukov et al.[8] in CCl_4.

radical cations and to estimate the conformational preferences of the poly[3,4-bis(ethylmercapto)thiophene] (PBEMT) and poly[3-(ethylmercapto)thiophene] (PEMT) systems. Most calculations were done by the method of partial retention of diatomic differential overlap (PRDDO).[13,14] PRDDO is an approximate molecular orbital treatment which accurately reproduces the results of minimum basis set ab initio calculations in a fraction of the computational time. Open-shell calculations were performed within the unrestricted Hartree–Fock (UHF) approximation.[15] The accuracy of the PRDDO method has been well-documented.[16,17] To check the accuracy of the PRDDO results in these systems, some calculations at the ab initio level were also performed by using the STO-3G[18] and STO-4-31G[19] basis sets and the ab initio program GAMESS.[20]

Band structure calculations were performed on polythiophene (PT), PEMT, and PBEMT. The extended Hückel approach within the tight binding approximation was employed.[21–27] This technique, more commonly known as the Mulliken–Wolfsberg–Helmholtz technique,[28] employs an empirical Hamiltonian representing the one-electron energy. The energy expectation values were evaluated by using a linear combination of atomic orbitals (LCAO). Briefly, the set of all energy bands obtained from the solution of the secular equation

$$H(k)C_n(k) = S(k)C_n(k)E_n(k)$$

describes the band structures of the one-dimensional polymer chain, where $H(k)$ is the Hamiltonian operator, $S(k)$ is the overlap matrix, and the $C(k)$ is the expansion coefficient in LCAO. The Hamiltonian operator is defined as

$$H_{ij} = KS_{ij}(E_{ii} + E_{jj})/2$$

where K is a scaling factor (usually 1.75) and E_{ii} denotes the one-electron eigenvalue. Due to symmetry considerations the energy bands are calculated within the first Brillouin zone, $-0.5K \leq k \leq 0.5K$ (where $K = 2\pi/a$ is the reciprocal lattice vector and a is the basis vector of the translational symmetry, which is parallel to the chain axis). The geometric parameters required, such as bond lengths and bond angles, were obtained from the PRDDO optimization of the raw crystallographic data. All the valence atomic orbitals of the H, C, and S atoms were included in the present calculation. The atomic parameters used for the calculations were obtained from the literature.[22,25] The polythiophene backbone was assumed to be planar for the calculations reported in detail. A few additional calculations were done with nonplanar backbones.

Oxidative Doping of Polymers. Solution preparation for UV–vis–near-IR oxidation studies were all done under a nitrogen atmosphere. Polymer solutions (0.05 mg/mL) were made in chloroform. The oxidizing agent nitrosyl hexafluorophosphate ($NOPF_6$) was used as received from Strem Chemicals and dissolved in dry CH_3CN (40 mg/mL). Oxidized polymer solutions were prepared by adding appropriate amounts of $NOPF_6$ solution to the previously prepared chloroform solutions of polymer. Electronic spectra were obtained on Cary 14 and Varian 2300 spectrophotometers.

Optoelectrochemistry experiments[29] were done in $CH_3CN/AgClO_4$ (0.1M) after solution casting the polymers on indium tin oxide (ITO) plated glass. The films was dried at 100 °C for 30 min. The optoelectrochemical cell consisted of the polymer cast ITO glass working electrode and silver foil counter electrode in a quartz cuvet. The potential was controlled between 0.0 and 1.0 V by using a Kikusui Model PAB 18-3A power source. After a small potential step the current was monitored and allowed to fall to background levels before spectra were obtained.

Complete solution oxidation of the polymers by $NOPF_6$, Br_2, and I_2 was carried out in chloroform. In the case of PEMT, an equimolar mixture of oxidizing agent per monomeric unit was prepared while, for PBEMT, five times as much $NOPF_6$ was required. The reaction was allowed to proceed for 10 min and solid oxidized polymer was isolated by vacuum filtration and washed with chloroform. The solids, as dark blue-black powders, were dried in a vacuum desiccator.

Electrochemistry. Cyclic voltammetry was performed in propylene carbonate (0.1 M) tetrabutylammonium tetrafluoroborate by using an EG&G PAR Model 273 potentiostat/galvanostat, a platinum button working electrode, a silver wire quasi-reference electrode, and a platinum foil counter electrode. Polymers were solution cast onto the platinum working electrode.

Molecular Weights. Molecular weights were determined by gel permeation chromatography (GPC) against polystyrene standards using a Waters 840 system and tetrahydrofuran as the eluting solvent. Ultrastyragel columns (Waters), with porosities of 10 000, 5000, and 100 Å in series, were used.

Conductivity Measurements. Measurements were made by either a two-probe method using a Keithly 610C Electrometer or a four-probe method using a Keithley 197 autoranging microvolt DMM. Samples were prepared by pressing between two copper wires in a capillary tube or as pressed pellets.

Results and Discussion

Monomeric Materials. The synthesis and characterization of BEMT has been well-documented by Yabukov et al.[9] EMT was synthesized in a similar manner, giving a clear oil [bp 81–83 °C (11 mmHg)]. The IR and NMR

Table III
Carbon-13 NMR Chemical Shift and Assignments for Monomeric and Polymeric Materials (ppm)

	α-C	β-C	$-CH_2-$	$-CH_3$
EMT	129.61	125.88	29.23	14.59
	123.17	131.78		
dibromo-EMT	110.89	132.32	29.30	14.81
	113.07	135.59		
PEMT	130–135 (br)		29.30	14.83
BEMT	123.14	133.48	28.29	14.12
diiodo-BEMT	90.89	140.83	30.78	14.64
PBEMT	135.05	137.78	30.71	14.57

data given in Tables I–III are consistent with the structures of these materials.

The halogenation of the above compounds is reported here for the first time. Exhaustive bromination, shown in reaction 1, in the α-position of EMT gave a thick clear oil [bp 145–147 °C (11 mmHg)]. The iodination of BEMT, shown in reaction 2, resulted in a yellow crystalline solid that has a melting point of 124–125 °C. The purity and structure of these monomers were confirmed by IR and NMR results as shown in Tables I–III.

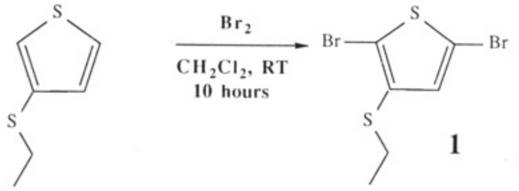

(1)

1

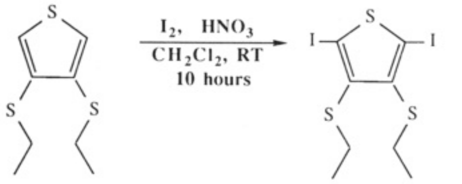

(2)

2

Polymerization Route. The polymerization route, using a Nickel-catalyzed Grignard coupling reaction shown in reaction 3, was selected after futile attempts at electropolymerizations. Electrooxidation in a number of solvent/electrolyte systems lead to formation of an orange, highly soluble, product and no precipitated or deposited polymer film. Other work in our laboratory[30] has demonstrated that a necessary condition for the successful polymerization of these and similar monomers (e.g., pyrrole) is that the spin density of the radical-cation monomers be located predominantly on the α-carbons of the heterocyclic ring. The calculated spin densities for EMT and BEMT at the PRDDO–UHF level are shown in Figures 1 and 2, respectively. Clearly, neither monomer has significant positive spin density at *both* α-carbons. This is entirely consistent with the observed failure of the electrochemical polymerizations. Calculations carried out on thiophene, bithiophene, and 1,2-dithienylethylene[31] all show significantly more spin density on the outer α-positions. These monomers are easily electropolymerizable to electrode deposited conductive polymer films. These examples show that, in a general sense, the determination of spin densities on these aromatic heterocycles can be used to discern whether or not a specific monomer will successfully electrochemically polymerize. Recently, Kaeriyama et al.[8] have electrochemically polymerized a structurally similar monomer, 3-(methylmercapto)thiophene, and obtained solid films. The materials were found to be oligomers with degrees of polymerization of 7.4, while under similar conditions 3-methoxythiophene electrochemically polymerizes to a higher degree of polymerization of 79. This order of magnitude increase in chain length, with change of heteroatom, demonstrates the lower reactivity of the mercapto-substituted monomer radical cation to polymerization.

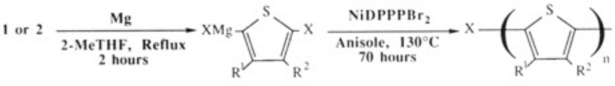

3. $R^1 = H$, $R^2 = EtS$; X = Br (3)
4. $R^1 = R^2 = EtS$; X = I

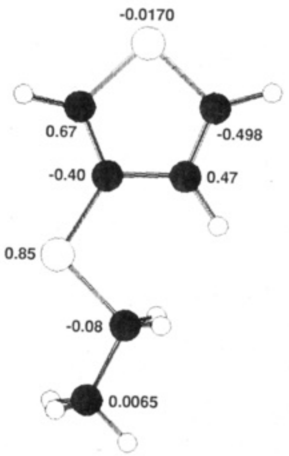

Figure 1. Radical cation spin density for 3-(ethylmercapto)thiophene.

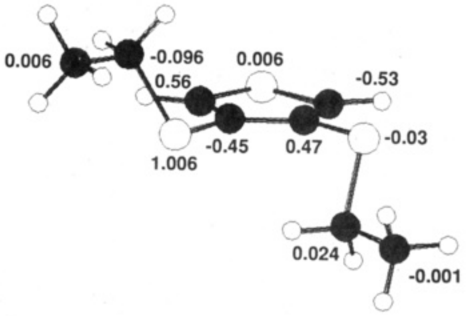

Figure 2. Radical cation spin density for 3,4-bis(ethylmercapto)thiophene.

Polymer Structural Properties. The principal IR absorption bands for the polymers and their assignments are listed in Table I. Results for polythiophene (PT) and poly(3-hexylthiophene) (P-3-HT) are reported for comparison. The absorbances due to the ring vibrations found in the vicinity of 1520–1440 cm^{-1} and the C–H out of plane vibrations about 820 cm^{-1} are characteristic of 2,3,5-trisubstituted thiophenes.[32] PBEMT does not exhibit any absorbances at 820 cm^{-1} since no thiophene ring hydrogens are present. The aromatic C–H stretch at 3070 cm^{-1} observed in PEMT is due to the β-position hydrogen. Weak bands at 3090 cm^{-1} are present in both the PEMT and PBEMT polymers, which can be attributed to the terminal hydrogens on the polymer chains which are located in the α-positions. This band is not observed for PT and P-3-HT, both reported previously and prepared in our laboratory, suggesting lower molecular weights for our polymers.

^1H NMR results are listed in Table II for the polymer. There is no significant shift in the resonance upon going from nonhalogenated monomers to polymers while splitting, due to proton coupling, is affected. Well-defined triplets and quartets are observed for the methyl and methylene substituents in the monomers which are transposed into broad peaks for the polymers. This can be attributed to the inequivalent proton environments for

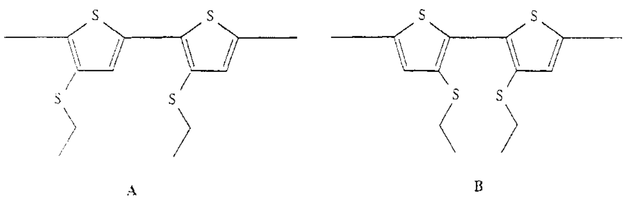

Figure 3. Head to tail (A) and head to head (B) linkages for poly[3-(ethylmercapto)thiophene].

the substituents along the polymer chain. The presence of two resonances for both the methyl and methylene groups in PEMT correspond to a mixture of head to tail and head to head linkages along the chain. The amount of these linkages, shown in Figure 3, is not controlled in this synthesis. This is not a factor for PBEMT which is structurally symmetric. The aromatic proton resonances prove that a straight chain 2,5-thienylene polymer is formed, and the weak resonances found for both polymers at 7.04 to 7.05 ppm are due to the α-position hydrogens of the chain ends.

The ^{13}C NMR chemical shifts and their assignments found in Table III, confirm the stability of the thiophene ring and the ethylmercapto substituents to the polymerization conditions. Two resonances are observed for the methylene group in PEMT, comparable to the ^1H NMR spectra, due to the different interchain linkages. A broad absorption in the aromatic region suggests numerous environments for the carbon nuclei of the thiophene rings. No other carbon nuclei are observed unlike the desulfurization of thiophene reported in the materials prepared by Kobayashi et al.[12]

Elemental analysis results are as expected for both polymers having atomic ratios of $C_{6.0}H_{5.9}S_{1.9}$ and $C_{8.0}H_{9.6}S_{3.0}$ for PEMT and PBEMT, respectively.

Polymer Physical Properties. Similar to previously reported 3-substituted thiophene polymers,[3,4,7] the neutral states of both PEMT and PBEMT are soluble in common organic solvents, including methylene chloride, chloroform, carbon tetrachloride, and tetrahydrofuran. These polymers, however, are not soluble in more polar solvents such as methanol, acetone, and water. Both polymers can be cast from solution onto mercury to form free standing, yet brittle, films. Means by which a film's mechanical properties can be improved are currently under investigation.

The number average molecular weights determined by gel permeation chromatography are 2200 (M_w = 13 000) for PEMT and 2600 (M_w = 9000) for PBEMT. This gives an average of about 15 repeat units for each polymer with a relatively broad polydispersity. These values should only be taken as approximate since it is common knowledge that comparison of polystyrene standards with conjugated polymers does not provide exact results. Difficulties in attaining a stoichiometric formation of active Grignard coupling sites is the expected problem in attaining high molecular weights since the polymers remain soluble throughout the polymerization.

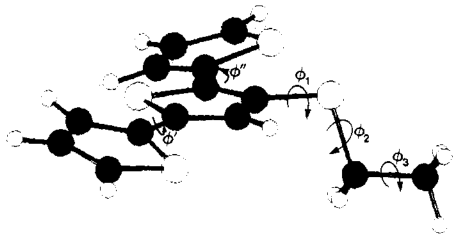

Figure 4. 3-(Ethylmercapto)-substituted thiophene trimer used in conformational analysis. ϕ' and ϕ'' are the torsional angles between rings. ϕ_1, ϕ_2, and ϕ_3 are the torsional angles of the C–S, S–C, and C–C bonds of the ethylmercapto substituent respectively.

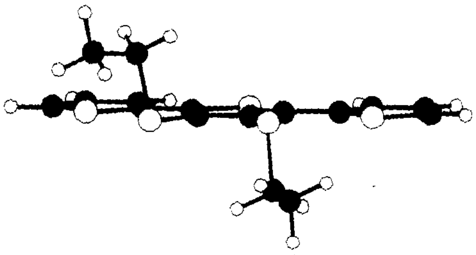

Figure 5. 3,4-Bis(ethylmercapto)-substituted thiophene trimer used in conformational analysis. Similar notations are used for the torsional angles as specified in Figure 4.

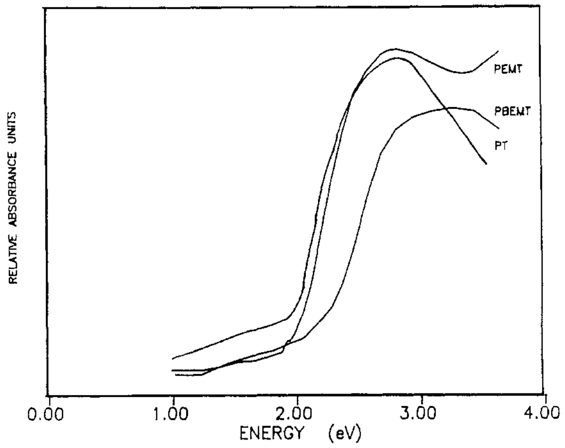

Figure 6. Optical absorption spectra of PEMT, PBEMT, and PT in the reduced (or neutral) solid form.

Polymer Conformations. In order to gain some insight into the preferred conformations of PEMT and PBEMT, PRDDO calculations were performed on the fragments shown in Figures 4 and 5. These models were chosen because they are the smallest systems which contain all of the steric and electronic interactions expected to be important in the real polymeric systems. The all transoid conformations were adopted, since both ab initio STO-3G and STO 4-31G calculations predict bithiophene to be more stable in this conformation. Referring to Figure 4, a potential energy surface was generated, at the PRDDO level for a planar backbone ($\phi' = \phi'' = 0°$), by varying ϕ_1 and ϕ_2 by 30-deg increments and optimizing ϕ_3 at each point. Only one minimum was found, which was subsequently refined to yield $\phi_1 = 72°$ and $\phi_2 = 13°$. This is a shallow minimum, and the all-planar configuration ($\phi_1 = \phi_2 = 0°$) is only 1.7 kcal/mol higher in energy. Subsequent optimizations of ϕ' and ϕ'' yielded 5° and 0°, respectively; however, this potential is extremely shallow. The structure with a planar backbone ($\phi' = \phi'' = 0.0$, $\phi_1 = 72°$, $\phi_2 = 13°$) is calculated to be only 0.06 kcal/mol higher in energy. This small energy difference may well be numerically insignificant.

Similar calculations were carried out for PBEMT (Figure 5). Here, the steric requirements of the ethylmercapto groups force one to lie above and one below the plane of the polymer, and the all-planar structure ($\phi_1 = \phi_2 = \phi' = \phi'' = 0$) lies several hundred kcal/mol higher in energy than the minimum. Optimizations were performed assuming $\phi_1 = -\phi_1'$, $\phi_2 = -\phi_2'$, and $\phi' = -\phi''$. The final optimized values are $\phi_1 = 78°$, $\phi_2 = 11°$, and $\phi' = 15°$.

Band Gap and Polymer Oxidation. The electronic spectra (vis–near-IR) were obtained for the polymers at various levels of oxidation in solution and as films cast on ITO glass. Figure 6 shows absorption spectra of neutral solid films of PEMT and PBEMT in comparison to that of reduced polythiophene (from 2,2′-bithiophene electro-

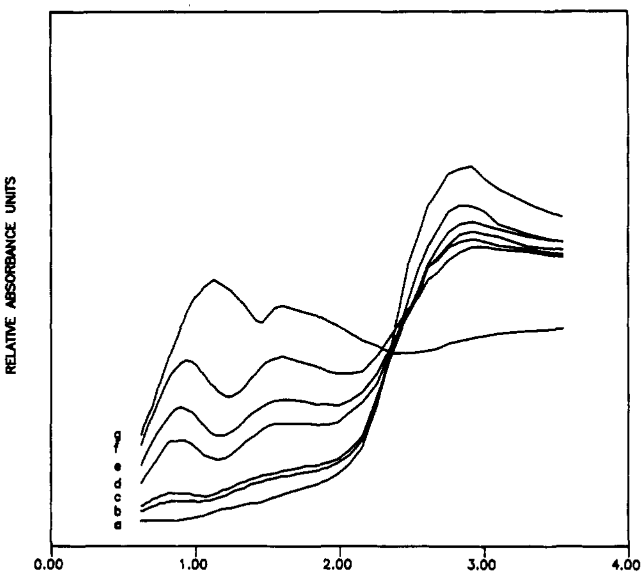

Figure 7. Solution doping of poly[3-(ethylmercapto)thiophene] with $NOPF_6$ in $CHCl_3$: (a) $y = 0.00$, (b) $y = 0.04$, (c) $y = 0.08$, (d) $y = 0.12$, (e) $y = 0.16$, (f) $y = 0.32$, (g) $y = 1.00$.

polymerized onto ITO glass). The mono β-substituted polymer PEMT presents a band gap (onset of the $\pi \rightarrow \pi^*$ transition) at about 2.0 eV which is comparable to that of polythiophene. The di-β-substituted polymer PBEMT presents a slightly higher band gap due to the presence of the two bulky ethylmercapto substituent causing a distorted preferred conformation.

The electronic spectra of these same polymers in solution shows a hypsochromic (blue) shift compared to their solid phase, 2.2 eV for PEMT and 2.4 eV for PBEMT. This shift implies a change to a more disordered, flexible conformation in solution.[5] Both polymers were oxidized in solution via the incremental addition of $NOPF_6$ oxidizing agent. The absorption spectrum for a neutral and oxidized PEMT polymer solution is shown in Figure 7. The molar ratio of dopant to monomer repeat unit, commonly termed the y value for $[(C_6H_6S_2)(PF_6)_y]_x$, is increased to a point (Figure 7g) where $y = 1$, assuming complete reactivity of the oxidizing agent. The $\pi \rightarrow \pi^*$ transition is depleted as two new lower energy bands start to grow. The two principle subgap absorptions with maxima at ca. 1.55 and ca. 0.85 eV in the doped polymer are consistent with charge storage predominantly via bipolarons.[33] As the dopant level is increased, the subgap absorptions are shifted slightly toward higher energies as seen in other polythiophenes. This can be attributed to depletion of electron density from the gap edge.

An optoelectronic study of PEMT film, cast on ITO glass, Figure 8, shows that both doping techniques give essentially the same results. The onset of the $\pi \rightarrow \pi^*$ transition is now found at ca. 2.0 eV with the two subgap transitions still at ca. 0.85 and ca. 1.55 appearing upon doping with the depletion of the interband transition. The striking similarity of these results indicate that, chemically or electrochemically, the species formed during oxidation are equivalent.

A similar set of oxidative doping experiments were carried out on PBEMT. In solution, spectra essentially equivalent to those obtained for PEMT were obtained, but excessive amounts of $NOPF_6$ oxidant were required ($y > 2$). The apparent excess addition of oxidant, with no visible sign of unreacted nitrosonium ion, suggests that the $NOPF_6$ may be reacting with the sulfur of the side chain. In the case of PBEMT, no changes in its absorption spectra were obtained during electrochemical oxidation. A possible explanation here is that the high content of ethylmercapto side groups is inhibiting charge transport through the material. This is addressed further in our discussion of bulk electrical conductivity.

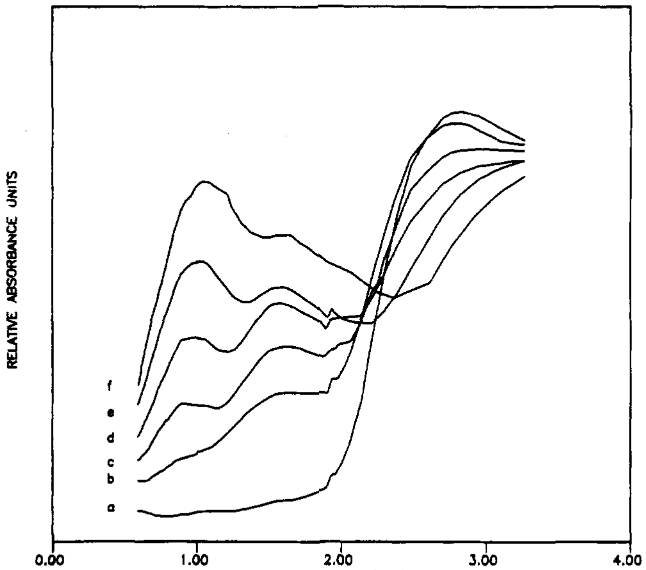

Figure 8. Optoelectrochemistry of poly[3-(ethylmercapto)-thiophene] with $AgClO_4$ in acetonitrile: (a) 0.00 V, (b) 0.09 V, (c) 0.21 V, (d) 0.30 V, (e) 0.42 V, (f) 0.54 V.

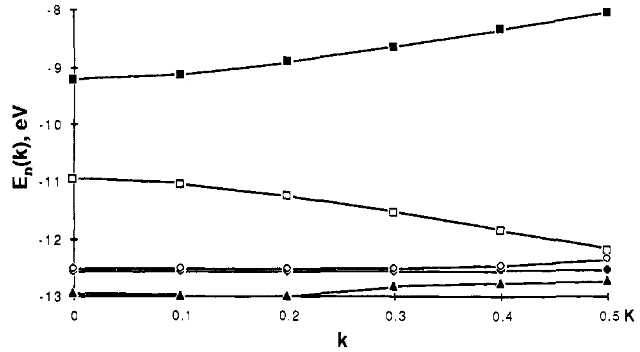

Figure 9. Energy bands as a function of wave vector, **k**, in the first Brillouin zone for polythiophene. Four top most filled valence bands (π) along with the lowest unoccupied conduction (π*) band are displayed.

It has been found that, as the length of the side group is increased, polymer solubility also increases. If solubility is mainly attributable to solvent/side chain interactions, little solvent effect should be discernible in the $\pi \rightarrow \pi^*$ transition energy. In fact, spectra of PEMT run in CCl_4 ($\epsilon = 2.24$), $CHCl_3$ ($\epsilon = 4.81$), THF ($\epsilon = 7.58$), and CH_2Cl_2 ($\epsilon = 8.93$) were identical. As the molecular weight of the polythiophene backbone increases the polymer solubility conversely decreases. Since high molecular weight is not necessarily required for conductivity in these samples, it is expected that these low molecular weight soluble polymers will be useful in blends and composites with high molecular weight carrier polymers.[34]

Band Structure Calculations. Standard extended Hückel calculations have been found to reproduce band structures of hydrocarbon polymers[21-27] fairly well. Initially, two chemical units of thiophene in the trans form were chosen as a repeat unit for unsubstituted polythiophene. The energy bands were calculated within the first Brillouin zone and are illustrated in Figure 9. Four highest occupied valence bands along with the lowest unoccupied conduction band are shown. The valence

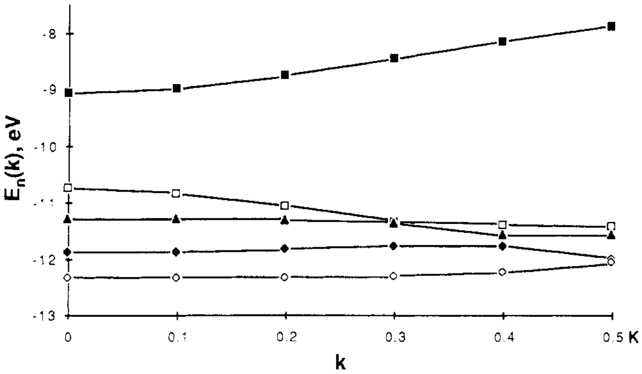

Figure 10. Energy bands as a function of wave vector, **k**, in the first Brillouin zone for poly[3-(ethylmercapto)thiophene]. Four topmost filled valence band (π) along with a conduction band (π^*) are shown.

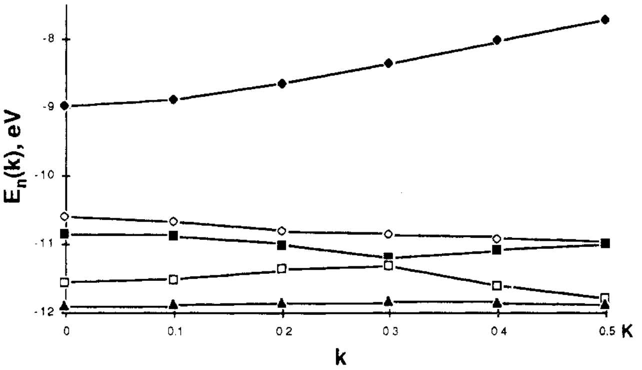

Figure 11. Energy bands as a function of wave vector, **k**, in the first Brillouin zone for poly[3,4-bis(ethylmercapto)thiophene]. Four topmost filled valence bands (π) and the lowest unoccupied conduction band (π^*) are displayed.

bands are mainly of π character, arising from the p_z orbitals of carbon and sulfur. The conduction band is of antibonding π^* character. The energy gap (which is the minimum separation between the highest occupied valence band and the lowest unoccupied conduction band) was found to be 1.74 eV, in good agreement with the experimentally accepted value of 2.0 eV. Our calculated bandwidth (BW) of the highest occupied band is 1.2 eV. For comparison, VEH calculations yield a band gap of 1.6–1.7 eV and a BW of 2.4–2.6 eV.[35]

In a similar manner, two chemical units of EMT and BEMT were chosen as the repeat units for the band structure calculations. The corresponding energy bands for the planar forms of the polymers are shown in the Figures 10 and 11. The energy gaps are calculated to be 1.67 and 1.60 eV for PEMT and PBEMT, respectively. These values are in reasonable quantitative agreement with the experimental findings discussed above. The calculated band gaps are quite sensitive to the twist angle (ϕ' and/or ϕ'') assumed. For instance, assuming $\phi' = \phi'' = 10°$ results in calculated band gaps of 1.87 and 1.73 eV for PEMT and PBEMT, respectively. Thus, the experimentally observed trends between solutions and the solid phase are probably a measure of the conformational preferences of the polymer backbone and the electronic effects of the substituents are negligible.

In the case of PT, the highest occupied valence band and the lowest unoccupied conduction band are exclusively comprised of p_z orbitals of carbon and sulfur atoms and are purely π in nature. The ethylmercapto substituents lead to a significant mixing of 3s and 3p orbitals on the sulfur atoms of the ethylmercapto groups with the polythiophene orbitals. The dispersions of the highest occupied valence bands of PEMT, and PBEMT are of the order of 0.67 and 0.37 eV, respectively. Thus, the highest π-band is much narrower in PEMT and PBEMT than in PT.

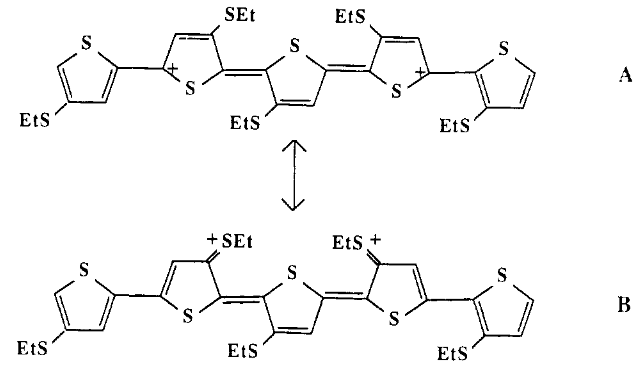

Figure 12. Possible resonance forms for a doubly charged bipolaronic carrier on poly[3-(ethylmercapto)thiophene].

Table IV
Electrical Conductivity for Neutral and Oxidized Polymers (Ω^{-1} cm^{-1})

	neutral	oxidized		
		NOPF$_6$	Br$_2$	I$_2$
PEMT	2×10^{-12}	2×10^{-5}	1×10^{-5}	1×10^{-3}
PBEMT	2×10^{-3}	2×10^{-7}		

Electrochemistry. Cyclic voltammograms were obtained against silver wire quasi-reference electrodes for both polymers. Oxidation potentials of 0.8 V for PBEMT and 0.75 V for PEMT were found. These values are comparable to the reported 0.7 V for poly(2,2′-bithiophene) and 0.77 V for poly(3-methylthiophene) (versus SCE).[1] Scanning to higher oxidative potentials resulted in the evolution of other peaks and loss of electroactivity. This may be due to the decomposition of the substituted thiophene repeat unit or side chain cleavage. These phenomena have been investigated more fully and will be reported elsewhere.[36]

Electrical Conductivities. As synthesized, both PEMT and PBEMT are insulating polymers as shown by the conductivities reported in Table IV. Reaction of polymer solutions with either NOPF$_6$, Br$_2$, or I$_2$ oxidants leads to precipitation of green/black semiconductive complexes in the form of insoluble powders. Though, as shown in Table IV, up to a 9 orders of magnitude conductivity increase is seen in the case of PEMT, the values of 10^{-5}–10^{-3} Ω^{-1} cm^{-1} are lower than that observed for the 3-alkyl-substituted thiophenes. An elemental analysis of Br$_2$-doped PEMT indicates that a relatively high dopant level is attained with about one Br$_3^-$ for every four thiophene rings. A higher conductivity of 4×10^{-1} Ω^{-1} cm^{-1} was measured for a Br$_2$-doped unsubstituted polythiophene by using comparable techniques.

The comparison of the conductivities of these, with related polymers, allows some generalizations to be made. The alkylmercapto-substituted polythiophenes have lower conductivities than their alkyl- or unsubstituted analogs in this, and other,[3,8] work. One possibility for this is the nature of the charge carrier.

The commonly accepted bipolaronic charge carrier in these α,α'-linked polyheterocycles is shown in Figure 12A for the specific case of the ethylmercapto polythiophene. It can be seen that another possible resonance form, Figure 12B, might exist in which the positive charge is localized on the sulfur atoms of side chains. We have carried out charge density calculations on these two charged structures and find that neither is dominant and the charge appears to be spread over the entire structure. Thus, a significant fraction of the positive charge may be centered on the ethylmercapto side chain. This charge is more localized and could serve to decrease carrier mobility in the polymer. Examination of the bipolaronic structure for PBEMT indicates that charge localization on the substituent sulfur atoms is also likely.

It was recently reported[37] that *cis*-polyisoprene, a nonconjugated polymer with isolated double bonds, could attain conductivities as high as $10^{-2}\ \Omega^{-1}\ cm^{-1}$ when subjected to I_2 doping. These charges, localized due to the lack of conjugation, are mobile via hopping processes. Similar charge hopping may be occurring in the polymers investigated here where the charge is somewhat localized on the sulfur atoms. This model can serve to explain the low conductivities measured in PEMT while the optical absorption experiments definitely show the presence of bipolarons. It should be pointed out that this resonance form only exists in the presence of head–head linkages along the chain where the substituted β-carbons are adjacent to one another.

Chemically synthesized,[3] I_2 doped, and electrochemically synthesized[8] poly[3-(methylmercapto)thiophene) (PMMT) has a reported conductivity of $10^{-1}\ \Omega^{-1}\ cm^{-1}$: 2 orders of magnitude higher than the maximum reported for PEMT here but still 4 orders of magnitude lower than the highest value reported for poly(3-methylthiophene).[38] The similarity in structure between PMMT and PEMT suggests reasons other than charge localization may be causing the lowered measured conductivities in PEMT. The number of possibilities is quite broad including molecular weight, morphology, and extent of oxidation. For example, we have found large differences in the electrochemical charge transport properties of poly(3-methylthiophene), when synthesized under varied experimental conditions, which can be explained by the morphology of the films obtained.[39]

Oxidation level also deserves strong consideration in that it is commonly known that conductivity is a function of dopant level. Recent work[36,40,41] has shown that over oxidation causes a loss of electroactivity in polythiophenes in general, and this effect was observed as a conductivity decrease for poly(3-methylthiophene) in highly doped samples. To evaluate this in the case of PEMT, we carried out a series of I_2 doping experiments reducing the amount of I_2. In these experiments only a decrease in conductivity was observed suggesting over oxidation is not limiting charge transport here.

The conductivity of PBEMT when doped is lower than PEMT. This is comparable to other dialkyl-substituted polythiophenes[3] and can, in addition to the effects described above, be attributed to a greater degree of steric hindrance between substituents forcing the chain partially out of planarity and inhibiting interchain packing of neighboring polythiophene chains. Figure 5 illustrates this latter possibility by showing the necessity of the two substituents of being on opposite faces of the thiophene ring. When this occurs in a polymer, it is difficult for the π systems of two chains to interact.

Conclusion and Summary

Poly[3-(ethylmercapto)thiophene) and poly[3,4-bis(ethylmercapto)thiophene] are both soluble conjugated polymers in the reduced state, with structures composed of 2,5-thienyl linkages. The Grignard coupling polymerization method affords materials that can be cast into free standing films, though structural and physical analyses indicate a relatively low degree of polymerization (15–20). This low DP is not necessarily a problem in that both polymers exhibit bipolaronic charge carriers upon oxidation and elevated conductivities. Comparison of the doped conductivities of PEMT ($10^{-3}\ \Omega^{-1}\ cm^{-1}$) with poly(3-alkylthiophenes) show the former to be ca. 3–6 orders of magnitude lower. One possible explanation for this is partial positive charge localization onto the sulfur atom of the ethylmercapto substituent. Theoretical analyses indicate that the polymers minimum energy conformations lead to planar conjugated backbones with some distortion in the disubstituted material. The calculated band gaps using the extended Hückel technique approximate those found experimentally and show little, if any, substituent effects. Thus differences between the spectra of polymers in solution and solid polymer films can be attributed to conformational changes.

Acknowledgment. This work was supported by grants from the Defense Advanced Research Projects Agency, monitored by the Office of Naval Research, and the Robert A. Welch Foundation.

Registry No. 1, 117896-78-3; 1 (homopolymer), 117896-87-4; 2, 117896-79-4; 2 (homopolymer), 117896-88-5; 3, 117939-36-3; 4, 117896-89-6; Ni(DPPP)Br_2, 15629-93-3; $NOPF_6$, 16921-91-8; 3-(ethylmercapto)thiophene, 6911-36-0; 3,4-bis(ethylmercapto)thiophene, 66820-73-3.

References and Notes

(1) Reynolds, J. R. *Mol. Elec.* **1986**, *2*, 1.
(2) Skotheim, T. J., Ed. *Handbook of Conducting Polymers*; Marcel Dekker: New York, 1986.
(3) Elsenbaumer, R. L.; Jen, K. Y.; Oobodi, R. *Synth. Met.* **1986**, *15*, 169.
(4) Sato, M.; Tanaka, S.; Kaeriyama, K. *J. Chem. Soc., Chem. Commun.* **1986**, 873.
(5) Hotta, S.; Rughooputh, S. D. D. V.; Heeger, A. J.; Wudl, F. *Macromolecules* **1987**, *20*, 212.
(6) Nowak, M. J.; Rughooputh, S. D. D. V.; Hotta, S.; Heeger, A. J. *Macromolecules* **1987**, *20*, 965.
(7) Bryce, M. R.; Chissel, A.; Kathirgamanataan, P.; Parker, D.; Smith, N. R. M. *J. Chem. Soc., Chem. Commun.* **1987**, 466.
(8) Tanaka, S.; Sato, M.; Kaeriyama, K. *Synth. Met.* **1988**, *25*, 277.
(9) Yabukov, A. P.; Grigor'eva, N. V.; Belen'kii, L. I. *J. Org. Chem. USSR (Engl. Transl.)* **1978**, *14*, 593.
(10) Ongley, P. A., Ed. *Organicum: Practical Handbook of Organic Chemistry*; Addison-Wesley: Reading, MA, 1973.
(11) Barker, J. M.; Huddleston, P.; Wood, M. L. *Synth. Commun.* **1975**, *5*(1), 59.
(12) Kobayashi, M.; Chen, J.; Chung, T. C.; Moraes, F.; Heeger, A. J.; Wudl, F. *Synth. Met.* **1984**, *9*, 77.
(13) Halgren, T. A.; Lipscomb, W. N. *J. Chem. Phys.* **1973**, *58*, 1569.
(14) Marynick, D. S.; Lipscomb, W. N. *Proc. Natl. Acad. Sci. U.S.A.* **1982**, *79*, 1341.
(15) Pople, J. A.; Beveridge, D. L. *Approximate Molecular Orbital Theory*; McGraw-Hill: New York, 1970.
(16) Halgren, T. A.; Kleier, D. A.; Hall, J. H.; Brown, L. D.; Lipscomb, W. N. *J. Am. Chem. Soc.* **1978**, *100*, 6595.
(17) Throckmorton, L.; Marynick, D. S. *J. Comput. Chem.* **1985**, *6*, 652.
(18) Hehre, W. J.; Stewart, R. F.; Pople, J. A. *J. Chem. Phys.* **1969**, *51*, 2657.
(19) Ditchfield, R.; Hehre, W. J.; Pople, J. A. *J. Chem. Phys.* **1971**, *54*, 724.
(20) Dupuis, M.; Spangler, D.; Wendoloski, J. J. General Atomic and Molecular Electronic Structure System, National Resources for Computations in Chemistry, as modified by: Schmidt, M. W., North Dakota State University; Elbert, S. T., Iowa State University.
(21) Hoffman, R. *J. Chem. Phys.* **1963**, *39*, 1397.
(22) Whangbo, M. H.; Hoffmann, R. *J. Am. Chem. Soc.* **1978**, *100*, 6093.
(23) Whangbo, M. H.; Hoffmann, R.; Woodward, R. B. *Proc. R. Soc. London* **1979**, *A.366*, 23.
(24) Imamura, A. *J. Chem. Phys.* **1970**, *52*, 3168.
(25) Bhaumik, D.; Mark, J. E. *J. Polym. Sci., Polym. Phys. Ed.* **1983**, *21*, 1111.
(26) Nayak, K.; Mark, J. E. *Makromol. Chem.* **1985**, *186*, 2153.
(27) Nayak, K. *J. Mater. Sci.* **1986**, *21*, 2322.
(28) McGlynn, S. P.; Vanquickenborne, L. F.; Kinoshita, M.; Carrol, D. G. *Introduction to Applied Quantum Chemistry*; Holt, Rinehard and Winston: New York, 1972; Vol. 1, p 67.

(29) Chung, T. C.; Kaufman, J. H.; Heeger, A. J.; Wudl, F. *Phys. Rev. B: Condens. Matter* **1984**, *30*, 702.
(30) Black, D. A.; Marynick, D. S.; Poropatic, P. A.; Reynolds, J. R., unpublished results.
(31) Martinez, M.; Reynolds, J. R.; Basak, S.; Black, D. A.; Marynick, D. S.; Pomerantz, M. *J. Polym. Sci., Polym. Phys. Ed.* **1988**, *26*, 911.
(32) Hartough, H. D., Ed. *The Chemistry of Heterocyclic Compounds: Thiophene and its Derivatives*; Interscience: New York, 1952.
(33) Brêdas, J. L.; Street, G. B. *Acc. Chem. Res.* **1985**, *18*, 309. Brêdas, J. L.; Tehemans, B.; Inipiat, J. G.; Andre, J. M.; Chance, R. R. *Phys. Rev. B: Condens. Matter* **1984**, *29*, 6761. Brêdas, J. L.; Scott, J. C.; Yakushi, K.; Street, G. B. *Phys. Rev. B: Condens. Matter* **1984**, *30*, 1023.
(34) Hotta, S.; Rughooputh, S. D. D. V.; Heeger, A. J. *Synth. Met.* **1987**, *22*, 79.
(35) Riga, J.; Snauwaert, P. H.; DePryck, A.; Lazzaroni, R.; Boutique, J. P.; Verbist, J. J.; Bredas, J. L.; Andre, J. M.; Taliani, C. *Synth. Met.* **1987**, *21*, 223. Themans, B.; Andre, J. M.; Bredas, J. L. *Synth. Met.* **1987**, *21*, 149.
(36) Tsai, E. W.; Basak, S.; Ruiz, J. P.; Reynolds, J. R.; Rajeshwar, K. *J. Electroanal. Chem.*, submitted for publication.
(37) Thakur, M. *Macromolecules* **1988**, *21*, 661.
(38) Roncali, J.; Yassar, A.; Garnier, F. *J. Chem. Soc., Chem. Commun.* **1988**, 581.
(39) Reynolds, J. R.; Hsu, S. G.; Arnott, H. J. *J. Polym. Sci., Polym. Phys. Ed.*, submitted for publication.
(40) Ofer, D.; Wrighton, M. S. *J. Am. Chem. Soc.* **1988**, *110*, 4467.
(41) Krische, B.; Zagorska, M. *Synth. Met.*, in press.

Theory of Block Copolymer Solutions: Nonselective Good Solvents

Glenn H. Fredrickson*

AT&T Bell Laboratories, Murray Hill, New Jersey 07974

Ludwik Leibler

Laboratoire de Physico-Chimie Theorique, E.S.P.C.I., 75231 Paris Cedex 05, France.

Received June 9, 1988; Revised Manuscript Received August 16, 1988

ABSTRACT: A theory to describe microphase separation and radiation scattering of AB diblock copolymers dissolved in a good, nonselective solvent is presented. In spite of the neutrality of the solvent, we find that the ordered microphases are inhomogeneous in solvent concentration as well as in copolymer composition. This arises from the ability of excess solvent at the interfaces between microdomains to screen unfavorable A–B interactions. It is also demonstrated that, unlike the melt, the microphase separation transition (MST) in copolymer solutions corresponds to a very narrow region of coexistence between a solvent-rich disordered phase and a solvent-poor ordered phase. The important semidilute regime is treated in detail—our analysis incorporates excluded volume swelling, corrections to scaling, and nonclassical fluctuation effects. For large molecular weights, the volume fraction of copolymer at the MST is predicted to scale as $\phi_t \sim N^{-0.62}$. Our results are consistent with previous measurements on copolymers in neutral solvents and suggest new experiments.

I. Introduction

Block copolymers have fascinated polymer scientists for many years, primarily because of the diversity of morphologies they exhibit.[1,2] In addition to the lamellar, cylindrical, and spherical microphases that have been known for some time, recent experiments on multiarm copolymers have turned up a new "ordered bicontinuous double-diamond" morphology,[3] a cocontinuous minimal surface structure that had previously been encountered only in multicomponent fluids containing surfactants. The variety of ordered structures that block copolymers possess and the unique control that the synthetic chemist has in determining those structures renders block copolymers very useful in commercial applications. For example, copolymers are used in high-impact-resistant plastics, membranes, photoresists, and adhesives and as compatibilizing additives to blends.

There has been much progress in the past decade with regard to our ability to predict the conditions (i.e., temperature, molecular weight, and composition) under which a molten block copolymer will exist in a particular morphological state. Building on the pioneering work of Williams and Leary[4] and Meier,[5] Helfand[6,7] developed an elegant statistical mechanical theory that allows comparison of the free energies of the various ordered phases and subsequent determination of the phase diagram. Helfand's theory is believed to be most accurate in the limit of strong incompatibility between the components of the copolymer, which is achieved by appropriate choice of monomers and at low temperature or high molecular weight. The theory also simplifies in this "strong segregation limit", where the interfacial thickness between microdomains is small relative to the characteristic size of a domain and one can employ the so-called narrow interface approximation.[6,7] Some interesting alternative approaches for treating the strong segregation limit have recently been published by Semenov[8] and by Ohta and Kawasaki.[9] One key prediction common to all the strong segregation theories is that the characteristic period of the ordered microphases scales as $N^{2/3}$, where N is the number of statistical segments per copolymer molecule. This prediction arises from a competition between the interfacial free energy and the entropy penalty associated with the non-Gaussian configurations chains must adopt to avoid passing through an interface.

Another important regime in molten block copolymers corresponds to the "weak segregation limit", which encompasses the compositionally disordered phase and the various ordered phases at temperatures very near the *microphase separation transition* (MST).[10] The MST is an order–disorder transition (similar to the crystallization of a one-component liquid) at which a disordered block copolymer melt first develops spatially periodic compositional order on lowering the temperature. In the weak segregation limit the ordered phases are not well-developed in the sense that the amplitudes of the compositional variations are very small and the boundaries between microdomains are not sharply defined. It is also believed

0024-9297/89/2222-1238$01.50/0